

Molecular BioSystems

Accepted Manuscript



This is an *Accepted Manuscript*, which has been through the Royal Society of Chemistry peer review process and has been accepted for publication.

Accepted Manuscripts are published online shortly after acceptance, before technical editing, formatting and proof reading. Using this free service, authors can make their results available to the community, in citable form, before we publish the edited article. We will replace this *Accepted Manuscript* with the edited and formatted *Advance Article* as soon as it is available.

You can find more information about *Accepted Manuscripts* in the [Information for Authors](#).

Please note that technical editing may introduce minor changes to the text and/or graphics, which may alter content. The journal's standard [Terms & Conditions](#) and the [Ethical guidelines](#) still apply. In no event shall the Royal Society of Chemistry be held responsible for any errors or omissions in this *Accepted Manuscript* or any consequences arising from the use of any information it contains.



www.rsc.org/molecularbiosystems

High-throughput metabolomic approach to explore the regulation of mangiferin on metabolic network disturbances of hyperlipemia rats

Chengyan Zhou^a, Gang Li^b, Yanchuan Li^b, Liya Gong^b, Yifan Huang^b, Zhiping Shi^b, Shanshan Du^b, Ying Li^b, Maoqing Wang^b, Jun Yin^{*a} and Changhao Sun^{*b}

a Development and Utilization Key Laboratory of Northeast Plant Materials, Key Laboratory of Northeast Authentic Materials Research and Development in Liaoning Province, School of Traditional Chinese Materia Medica, Shenyang Pharmaceutical University, 103 Wenhua Road, Shenhe District, Shenyang 110016, China

b Department of Nutrition and Food Hygiene, School of Public Health, Harbin Medical University, 157 Baojian Road, Nangang District, Harbin, 150081, China

*Correspondence

1. Prof. Jun Yin

Development and Utilization Key Laboratory of Northeast Plant Materials, Key Laboratory of Northeast Authentic Materials Research and Development in Liaoning Province, School of Traditional Chinese Materia Medica, Shenyang Pharmaceutical University, 103 Wenhua Road, Shenhe District, Shenyang 110016, China

Tel/fax: +86-24-23986491; +86-0451-87502801. E-mail: junyin_good@163.com

2. Changhao Sun

Department of Nutrition and Food Hygiene, School of Public Health, Harbin Medical University, 157 Baojian Road, Nangang District, Harbin, 150081, China

Abstract:

This paper was designed to study metabolomic characters of the high-fat diet (HFD)-induced hyperlipemia and the intervention effects of Mangiferin (MG). In this study, we aimed to investigate the intervention of MG on rats with hyperlipemia induced by HFD and explore the possible mechanisms of hyperlipemia. Urine metabolic profiles were analyzed using ultra-performance liquid chromatography/electrospray ionization quadruple time-of-flight mass spectrometry (UPLC-ESI-QTOF-MS) coupled with the principal component analysis (PCA) and partial least squares-discriminate analysis (PLS-DA) models, Heatmap and metabolism pathway analysis. PCA was applied to study the trajectory of urinary metabolic phenotype of hyperlipemia rat after administration of MG. VIP-plot of orthogonal PLS-DA was used for discovering potential biomarkers to clarify mechanism of MG. Biochemical analyses indicate MG can alleviate the hyperlipemia damage. Twenty significantly changed metabolites (potential biomarkers) were found to be reasonable in explaining the action mechanism of MG. The effectiveness of MG on hyperlipemia is proved using the established metabolomic method and the regulated metabolic pathways involve TCA cycle, taurine and hypotaurine metabolism, glyoxylate and dicarboxylate metabolism, glycine and serine and threonine metabolism, glycerophospholipid metabolism, primary bile acid biosynthesis etc. The results indicated that MG has a favourable protective effect on HFD-induced hyperlipemia by adjust the metabolic disorders. It also suggests that the metabolomic technology is a powerful approach for elucidation of the action mechanisms of MG.

Keywords:

Mangiferin; metabolomics; UPLC-ESI-QTOF-MS; metabolites; hyperlipemia; urine

1. Introduction

Hyperlipidemia is a well-known major risk factor for several diseases, such as atherosclerosis, coronary heart disease (CHD), hepatic steatosis and diabetes, and is now becoming more common, because of the imbalanced energy dietary habit [1]. If hyperlipemia was diagnosed timely, and with proper dietary alterations and medications treatment, it can be well regulated and controlled [2]. However, anti-hyperlipidemia drugs (such as statin and fibrate, etc.) caused a number of adverse effects, including dementia risk, muscle-related adverse effects, low plasma vitamin D levels, creatin kinase elevations, derangements in hepatic function, etc [3]. Thus, the management of hyperlipidemia is still a major challenge with respect to patients who are intolerant to the adverse effects of these classic hypolipidemic drugs [4]. Phytochemicals are attracting increasing attention because of their health benefits and their relatively lower toxicity and might be suitable for long-term supplementation. Mangiferin (MG), a classic phytochemicals, is an active phytochemical present in various plants including *Mangifera indica* L., *Anemarrhena asphodeloides* Bge and etc. It has efficiently action for hyperlipemia rats [5,6]. However, pharmacological effects of MG against hyperlipemia focus on molecular biological techniques and biochemical analysis, and there are no reports on effect of MG on the urinary LC-MS-based metabolic profiling of hyperlipemia.

Metabolomics, a sensitive and novel technology, the small molecules global qualitative and quantitative measurement in biofluids, shows great promise as a means to identify biomarkers of drug efficacy. It has shown considerable potential in many applications involving disease diagnosis, studying global effects of genetic manipulation, drug metabolism and natural product discovery, etc [7-13]. Drug discovery and development is a field of considerable interests, the metabolic profiling can provide a global view of abundance changes of endogenous metabolites in monitoring cellular responses to perturbations of drug treatment [14]. Owing to its high chromatographic resolution, high sensitivity, and rapid separation, ultra-performance liquid chromatography (UPLC) coupled with mass spectrometry (MS) has been used widely in the systematic characterisation of drug targets, thereby helping to reduce the typically high attrition rates in discovery projects [15-21]. It is a more effective approach by computational integration of different knowledge sources and unprecedented opportunities are provided by plentiful metabolomic data for drug target identification[22].

The core idea of metabolomics is to determine the metabolites of relatively low-weight molecular, then to transform the data of metabolic profiles into useful information by pattern recognition tools, and to revealing the essence of diseases and assessing therapeutic effects of drug [23-26]. In the current study, we performed a urinary metabolomics study on MG treatment for hyperlipemia rats with multivariate statistics by ultra-performance liquid chromatography/electrospray ionization quadruple time-of-flight mass spectrometry (UPLC-ESI-QTOF-MS), and then identified the reliable biomarkers of hyperlipemia. This is the first study that obtains a systematic view of dissection of the urinary LC-MS-based metabolic profiling of MG as an effective treatment for hyperlipemia.

2. Materials and Methods

2.1. Chemicals and reagents

Acetonitrile (chromatographic grade) was purchased from Honeywell Burdick & Jackson (Muskegon, MI, USA). Formic acid (HPLC-grade) was obtained from Beijing Reagent Company (Beijing, China). Deionized water was prepared by Ultra Clear System in our laboratory (Siemens Water Technologies, Nuremberg, Germany). Leucine enkephalin was purchased from Sigma–Aldrich (St. Louis, MO, USA). All other reagents were HPLC grade. The assay kits for total cholesterol (TC), triglyceride (TG), high-density lipoprotein cholesterol (HDL-C), low-density lipoprotein cholesterol (LDL-C) were purchased from BioSino Bio-technology and Science Inc (Beijing, China). MG (>95%, HPLC) were purchased from Nanjing zelang pharmaceutical technology company (Nanjing, China).

2.2. Animal treatments

Sixty six 7-wk-old male SD rats (weighting 200 ± 20 g) were purchased from the Vital River Laboratory Animal Technology (Beijing, China). All rats were allowed to acclimatize in communal plastic cages for a week before the experiment beginning. Temperature and relative humidity were regulated at $21 \pm 2^\circ\text{C}$ and $55 \pm 5\%$, respectively. A cycle of 12 h light/12 h dark was established. A 12-h light/12h dark cycle was established, free access to standard diet and drinking water.

After a week of acclimatization, animals were randomly assigned to 2 groups: normal control group (NC, n =20), high-fat group (HF, n =46). Rats from the NC group were fed a normal diet, while rats in the HF group were fed a high-fat diet (HFD: 15% lard, 10% sucrose, 1% cholesterol and 74% standard chow.). After 5 weeks of feeding with these diets, the rats of the HF group were randomly divided into 2 groups: a high-fat control group (HF, n=20), a MG treatment group (HF+MG, n=20). MG was given by oral gavage in 0.5% carboxymethyl cellulose (CMC) buffer solution for 13 weeks, the dosages were 300mg/kg/day. Rats in the NC and HF groups were given by gavage with an equivalent volume of 0.5% CMC buffer. The rats were given an oral accurate volume of 1 mL/100 g of each rat. The rats in the NC group were fed the normal diet continuously, and rats in the other groups were fed the high-fat diet until the end of the experiment. To determine effect of MG treatment on hyperlipemia in high-fat-fed rats, we chose dynamic observation point at 5 and 11 week (before MG treatment, after 6 weeks MG treatment). At the every time point, six rats were sacrificed from each group randomly. After 13 weeks of MG treatment, all rats were sacrificed. The detailed experimental protocol was shown in Fig.S1.

All rats in the experiment were fasted for 12h before sacrifice, and then were anesthetized by pentobarbital. Blood samples were taken from the inferior vena cava. Serum was obtained by centrifuging the blood at 3000 rpm for 15 min at 4°C . Portions of livers were immersed in 10% neutral buffered formaldehyde for histological observation. The MG treatment on urinary metabolic study was divided into 3 time points, including 5, 10, 14 and 18 weeks (0, 5, 9 and 13 weeks after MG treatment). At the indicated time points, 24 h all rats urinary samples obtained from each groups were collected, respectively; then immediately centrifuged at 12,000 rpm and 4°C for 15 min, and the

supernatant was stored at -80°C until measurement. Fecal samples in each group were collected at 5, 11, 18 weeks. TC, TG, HDL-C, and LDL-C content were measured using an enzymatic kit (Applygen Technologies) following the manufacturer's instructions. Histological observation was performed in a blinded fashion by a experienced gastrointestinal pathology professor using the NAFLD histological scoring system [27]. The experimental procedures were approved by the Animal Care and Ethics Committee at Harbin Medical University (approval number: HMU-E-2013-08562).

2.3. Metabolic profiling

2.3.1. Sample preparation

Urine samples were dissolved at room temperature prior to analysis, diluted 1:1 (v/v) with deionized water, vortexed for 60s, and then centrifugation at 12,000 rpm for 15 minutes. The clear supernatant was then transferred to an autosampler vials and kept at 4°C . A 2 μL aliquot was made into the column in each run.

2.3. 2. UPLC conditions

UPLC-ESI-QTOF-MS measurement was performed on a 1.8 μm T₃ column (ACQUITY (HSS); Waters Corp., Milford, MA, USA) coupled to equipped Mass Spectrometer with the positive ion mode (ESI⁺), the negative ion mode (ESI⁻) (Waters Corporation, Manchester, UK) and a UPLC system (ACQUITY UPLC; Waters Corp., USA). The auto sampler and column temperatures were kept in 4°C and 35°C , respectively. The flow rate of the mobile phase was 350 μL /min. 0.1% formic acid were contained in the mobile phase (solution A [water] and solution B[acetonitrile]). The sample analytes were eluted from the column with a gradient elution. The elution gradient was as follow: 0.5–6 min, 2–25% buffer B; 6–9 min, 35–70% buffer B; 9–10.5 min, 70–98% buffer B; 10.5–12 min, 98% buffer B; 12–18 min, 2% buffer B.

2.3. 3. Mass spectrometry conditions

The analytical parameters were as follows: capillary voltage, 3000v(ESI⁺) and 2800 V (ESI⁻),and the sample cone voltage was40 V; collision energy, 6 eV; source temperature was set at 100°C ; desolvation gas (nitrogen) flow, 600 L/h (ESI⁺) and 650L/h (ESI⁻); desolvation gas temperature of 320°C was used; cone gas (nitrogen) flow of 50 L/h was set; collision gas,argon; MCP detector voltage, 2550V (ESI⁺) and 2200 V (ESI⁻). 0.48 seconds was set in the Q-TOF mass acquisition rate with an interscan delay of 0.1 second.From 50 to 1000 m/z was set at the scan mass range.In centroid mode, the Q-TOF MS/MS data were collected by the lock spray frequency to ensure accuracy and reproducibility. A concentration of 200 pg/ml leucine-enkephalin was used as lock mass in ESI⁺ and ESI⁻.The lock spray frequency was set at 8 seconds, and the lock mass data were averaged over 10 scans for correction.

2.3.4. Identification of biomarkers and metabolic pathway analysis

The UPLC-ESI-QTOF-MS raw data were analyzed by MarkerLynx Application Manager 4.1 (Waters Corporation, Milford, MA, USA). The identities of the specific metabolites were confirmed by comparison of their mass spectra

and chromatographic retention times with those obtained using commercially available reference standards. Databases (HMDB, KEGG) were used in the interpretation of the implicated pathways of biomarkers. Database source (KEGG, SMPD, METLIN) were used in the interactions, construction, and pathway analysis of potential biomarkers, then identified the affected metabolic pathways visualization and analysis.

2.4. Data analysis

All data are presented as mean±SD. The analysis of covariance (ANCOVA) was performed by SPSS (version 16.0; Beijing Stats Data Mining Co. Ltd., China). Test, $P < 0.05$ were considered the level of statistical significance.

3. Results

3.1 Effect of MG on serum metabolites

Hyperlipidemia, characterized by increased TG, TC, LDL-C levels and decreased HDL-C levels. The TG, TC, HDL-C, LDL-C levels were measured (Figure 1a, 1b, 1c, 1d). After 5 weeks, the TG, TC, LDL-C levels increased significantly in the HF group as compared to the NC group, whereas the HDL-C concentrations decreased significantly. After 11, 18 weeks, the TG, TC, LDL-C levels in the HF+MG group were obviously decreased and HDL-C were significantly increased compared to the HF group. These results suggest that the rats from the HF group are subject to significant hyperlipemia after 5 weeks, 11 weeks and 18 weeks in the high fat diet feeding, while the HF+MG group showed well recover from 11 to 18 weeks.

3.2 Effect of MG on liver lipid and histopathology

Rats in the HF group had significantly higher TG, TC levels and liver fatty droplets accumulation than rats in the NC group. MG treatment significantly decreased TG, TC levels and liver fatty droplets accumulation in rats fed a HFD (Figure 1e, 1f, 2a, 2b, 2c). H&E-stained also indicated the obvious inflammation and hepatic injury in the HF group than the NC and HF+MG group (Figure 2b).

3.3 Effect of MG on fecal TG, TC

HF group rats had significantly higher fecal lipid concentrations compared with the NC rats (Figure 1g, 1h). The lipid levels of fecal samples collected from the HF+MG group were significantly higher than rats in the HF groups ($P < 0.05$).

3.4 Metabolomic Analysis

3.4.1. LC-MS analysis of metabolic profiling

An initial overview of the quality of the analytical run was obtained by analysis of the sample dataset that included the QC injections. The stability of the metabolomics platform was excellent throughout the run, and was sufficient to ensure the data quality for further global metabolomics analysis. The general clustering trends were reaschered and depicted in NC and HF rats. The PLS-DA scores plot presented that (for the first two components, $R^2Y = 0.9141$ (ESI⁺) and $Q^2 = 0.8218$ (ESI⁺); $R^2Y = 0.5867$ (ESI⁻) and $Q^2 = 0.0860$ (ESI⁻); Figure 3a, 3b, 3c, 3d and attached list 2)

the rats of the NC and HF group could be separated into significant clusters, with remarkable metabolic perturbations between the NC group and HF group (Fig S2).

Urinary metabolic profiling of the hyperlipemia rats was performed by a metabolic trajectory analysis using PCA and PLS-DA from 1 to 18 weeks. The metabolic trajectory scores were set at dynamic and continuous in urinary metabolites during the initiation and progression of hyperlipemia (Figure 4a, 4b and Fig S3). The above results suggested three different developmental stages for the progression of hyperlipemia model, including three clear stage, such as the development early stage from 1 to 5 weeks, the middle development stage from 6 to 14 weeks and the late development stage from 15 to 18 weeks.

To investigate the effect of MG supplementation on the urinary metabolic profiling of hyperlipemia rats, the hyperlipemia rats were supplied with the MG (300mg/kg) after week 5. Thus, MG can inhibit hyperlipemia from the middle development stage to the late development stage. The PCA and PLS-DA score plots indicated that the MG rats gradually clustering trend with the NC rats, and significantly deviated from the HF rats (Figure 4c, 4d and Fig S4). MG continuous supplementation until 13 weeks, the MG rats clusters were completely discriminated from the HF rats, and were recovered gradually to the normal levels (Figure 4e, 4f and Fig S4).

OPLS-DA models were performed to identify the difference in metabolites between the NC and HF rats. The OPLS-DA score plots are shown in Figure 5a and 5b. The mass spectrometry signals responsible for discriminating variables were selected primarily according to their variable importance in projection values ($VIP > 4$) (Figure 5c, 5d) and S-plot by OPLS-DA (Figure 5e, 5f). Following the OPLS analysis, potential markers were extracted from S-plots, and markers were chosen based on the above protocol, were plotted at the top or bottom of the S plot. The OPLS-DA loading S-plot (Figure 5g, 5h), a plot of the covariance versus the correlation in conjunction with the variable trend plots, allows easier visualization of the data. The discriminating variables obtained from the OPLS-DA models were further validated by the Wilcoxon test ($P < 0.05$). Although hundreds of discriminating variables were selected as potential markers, only a small percentage was shared across different time points. The real biomarkers should be changed following the progression of hyperlipemia, therefore, only the biomarkers with regular change trends were considered as potential biomarkers. Based on the above protocol, 20 potential biomarkers associated with hyperlipemia were selected. The results were shown in the Table 1 with their corresponding retention time, accurate molecular mass, ion mode, related trends and information on the structural identification of these potential biomarkers.

In the 20 potential hyperlipemia biomarkers, 15 biomarkers were upregulated and 5 biomarkers were downregulated in the HF rats. To illustrate the identification of metabolites, we took the follow ion (retention time $t_R = 0.66$ min, m/z 124.0064) as an example to be described below (Figure 6a). According to the protocol detailed above, the ion has a high VIP value. This ion may contain an odd number of nitrogen atoms because its precise molecular weight is 124.0064, and its molecular formula was speculated to be $C_2H_6NO_3S$ based on the analysis of its elemental

composition and fractional isotope abundance. The main fragment ions that were analyzed via the MS/MS screening were observed at m/z 124, 265, 106, 95, 80, and 65, which could be the $[M-H]^-$ of lost-NH₃, -CH₃N, -C₂H₆N, -C₂H₅N, respectively. Finally, based on a database search, the ion was determined to be taurine.

3.4.2. Effect of MG on identification and quantitation of potential metabolites biomarkers

The relative mean height intensity of different metabolites of the NC rats, MG rats vs HF rats were shown in Figure 6b and 6c. The parallel heatmap visualization (Figure 6d, 6e) for the rats that treated with HF+MG and HF groups could be achieved the distinct segregation. The results indicated that the potential biomarkers were changed remarkable between the MG rats and the HF rats following the visual changes in the rats urinary metabolic profiling. According to the parametric t-test, compared with the alterations of hyperlipemia relative metabolites, most of them were reset to a healthier level and were reversed after MG supplementation. For example, the peak area of the biomarker with m/z 407.2779 in the MG rats decreased significantly at the end of week 5 and disappeared at the end of weeks 10. This was the representative hyperlipemia biomarker. If there were still significant differences in the peak areas of biomarkers between the HF+MG and NC rats after MG supplementation for 5 weeks, these biomarkers should be excluded from the biomarker list. The supposed molecular formulas were searched in Chemspider, KEGG and other databases, then the possible chemical structures were identified by comparing the possible chemical constitutions, MS/MS spectra and/or retention time against the reference standards.

3.4.3. Effect of MG on metabolic pathway analysis

In order to identify whether our observations of changes in the metabolites in the setting of MG treatment effect in fact reflected coordinate changes in defined metabolic pathways, MetPA software was used to identify network pathway. The detailed construction of the metabolism pathways of the Figure S5a-g and Table S1 is the pathway impact value calculated from pathway topology analysis 0.10 was set for the impact threshold value, then above this threshold, potential targets pathway were filtered out. Results suggested that these target pathways showed the remarkable perturbations over the time-course of MG treatment and could contribute to development of MG treatment effect.

4. Discussion

As shown by our experiments, HFD can produce the metabolic stress response, which resulted in dramatic alterations in hyperlipemia metabolism, but MG can regulate the change well. The change in the biochemical parameters and histology observation is consistent with the changes in the metabolic profiles in the serum and liver. The serum and liver TG, TC, LDL-C levels increased significantly in the HF group than in the NC group and HF+MG group (Figure 1; Figure 2). The PLS-DA scores plot presented that the NC rats and HF rats could be separated into significant clusters, the HF+MG rats graduated clustering trend with the NC rats.

Metabolomic approach have been utilized to further describe metabolic changes in the throughout experiment. 20

specific metabolites (Table 1) were relevant for the MG target discovery and the MG pathway-specific expression profiles researches, which indicated that unusual metabolism regulation occurred in the hyperlipemia rats. Identification and validation of MG target is the essential first step in MG research and development. The MG target is specific to a disease condition, which is a key molecule involved in a signaling pathway or particular metabolic. More importantly, we found that MG graduated regulation hyperlipemia by significantly activating 6 interconversions metabolic pathways, such as taurine and hypotaurine metabolism, glyoxylate and dicarboxylate metabolism, glycine and serine and threonine metabolism, TCA cycle, glycerophospholipid metabolism, primary bile acid biosynthesis. Among which, the TCA cycle is the central to energy metabolism in this network. The MG treatment designed to adjust the pathway function by regulation a key molecule or improve the influenced normal pathway by promoting specific molecules in the diseased state, and can change the global metabolic system by the above targets. In the present study, the biological relationships between the potential biomarkers and MG treatment effects of hyperlipemia rats are discussed according to the pathways shown in Figure 7.

The first pathway is taurine and hypotaurine metabolism. Taurine, one of the important asulphonic amino acids, is found ubiquitously in all mammalian tissues. Taurine, is the second most abundant in skeletal muscles and the central nervous system after glutamate, is higher than any other amino acids in the other tissues.²⁸ Taurine has several important physiological activities, such as bile acid conjugation, antioxidant activity, anti-inflammatory activity, maintenance of normal mitochondrial function, osmoregulation, neuromodulation, and ATP production.²⁹ Taurine also was originally described to inhibit lipid peroxidation.³⁰ At present, taurine has been demonstrated to inhibit the lipid accumulation in the liver.³¹ Moreover, taurine has been shown to decrease LDL cholesterol, accelerate cholesterol degradation and HDL levels elevation among individuals fed a high fat diet.³² Furthermore, taurine also reduces plasma triglyceride levels.³³ Overall, the increased in taurine in this study indicate that hyperlipemia could result the lipid accumulation of HF rats.

Taurine in body is provided by diet (especially fish and seafood), but also main derived endogenously from biosynthesis in liver. The biosynthesis of taurine is species-dependent, with hepatic synthesis being very active in rats.³⁴ In this synthesized process, cysteine sulfinic acid decarboxylase (CSAD) is the rate-limiting enzyme in the de novo biosynthesis of taurine.³⁵ The taurine is excreted by urine and bile acid conjugates. In according to the following primary bile acid biosynthesis, taurine in HF group wasn't enough by diet providing, then the CSAD activity was improved for taurine lack, whereas which wasn't enough to counteract the taurine lack too. Overall, taurine was decreased in HF group. Some studies indicated that reduced taurine levels were observed in HFD-induced obese mice,³⁶ which may also be the obesity-associated changes.³⁷ In this study, the intensity of urine taurine was significantly decreased in the HF group compared with the intensity in the NC group, indicating that hyperlipemia could promoted the CSAD activity. Urine taurine increases after MG administration, suggesting that MG can normalize the CSAD activity and counteract the negative effect of hyperlipemia on taurine formation.

The second pathway is glyoxylate and dicarboxylate metabolism. Glycine is the important intermediate of glyoxylate and dicarboxylate metabolism. Glycine and glyoxylate can be mutual converted by glutamate--glyoxylate aminotransferase in the glyoxylate and dicarboxylate metabolism. Glycine can also come from choline following a series of demethylation reactions.³⁸ In this study, the decreased choline indicated in the HF group that the more choline converted to the glycine, thus the glycine was increased. Choline normalized cholesterol metabolism, was sufficient to prevent lipids accumulation development and improve liver function in *Pemt/Ldlr* knockout mice fed a high-fat diet.³⁹ The decreased choline suggested that more lipids were accumulated in the liver in the HF group, but the increased choline in the HF+MG group indicated that MG can protect the liver function and inhibited the lipids accumulation in the liver.

Glycine is required for the biosynthesis of glutathione (GSH), protein, purines and DNA/histone methylation. GSH, a tripeptide comprising cysteine, glycine, and glutamate, is required to maintain the redox balance. The major function of GSH is to reduce soluble hydrogen peroxide and alkyl peroxides in tissues. GSH can be converted to glutamate and then α -keto-glutarate, α -Ketoglutarate is an anaplerotic intermediate that refuels the citrate cycle.⁴⁰ The pathway is a contributor of TCA intermediates; it is responsible for approximately half of the anaplerotic flux to the TCA cycle. Glycine also fuels heme biosynthesis and thus sustains oxidative phosphorylation.⁴¹ Citric acid is the one of TCA intermediates. Glycine and Citric acid is significantly increased in the HF group than the NC and HF+MG group in the urine, which indicated hyperlipemia can disturb GSH synthesis and the TCA cycle, on the contrary MG can regulate it well.

The third pathway is glycine and serine and threonine metabolism. Glycine, a nonessential amino acid, is the most simple structure in the body. Glycine and serine is the important intermediate of glycine and serine and threonine metabolism. Glycine is generated from serine and threonine by the enzyme serine hydroxymethyltransferase, threonine dehydrogenase and glycine C-acetyltransferase in the glycine and serine and threonine metabolism.⁴² Serine and glycine are biosynthetically linked, and together provide the essential proteins, nucleic acids, and lipids that are crucial to body health. Glycine has been shown to protect hepatocyte against hypoxia,⁴³ inhibited the lipids accumulation in the liver.⁴⁴ The significantly increased glycine in the HF group than the NC and HF+MG group in the urine, which indicated hyperlipemia can disturb glycine and serine mutually conversion in the body, so that glycine was increased. But MG can improve the mutually conversion of glycine and serine. Tyr-Ala-Phe can provide tyrosine and phenylalanine, then phenylalanine can form phenylacetate, which is a dietary polyphenols.⁴⁰ Phenylacetylglycine is typically produced from glycine conjugation with phenylacetate.⁴⁵ The urinary increased phenylacetylglycine indicated that abnormal lipids accumulation in the tissues.⁴⁶

Serine can convert tryptophan, then form xanthurenic acid by the enzyme catalysis. High excretion of urinary xanthurenic acid during inflammation has been observed in children with infections. Alternatively, xanthurenic acid may be involved in the induction of immune tolerance toward rheumatoid arthritis (RA) presumably. A recent study

showed that xanthurenic acid contributed to the induction of immune tolerance during allergen immunotherapy in a mouse model of allergic asthma.⁴⁷ In this study, the increased xanthurenic acid in the HF group, indicated that hyperlipemia can result in inflammation and damage in the liver, which is confirmed with histology observation in this study (Figure 2b). The level of xanthurenic acid in urine decreases after MG administration, suggesting that MG can inhibit inflammation progression.

The fourth pathway is the citrate cycle (TCA cycle). TCA is of vital importance for the survival of life, and plays an important role in gluconeogenesis, transamination, deamination and lipogenesis.⁴⁸ Acetyl-CoA is the starting point for the TCA cycle, and obtained from various sources.⁴⁹ Citric acid, succinic acid and fumaric acid are important intermediates of the TCA cycle. Citrate was converted from Acetyl-CoA by citrate synthetase. In this study, acetyl-CoA can be impaired by many pathways (taurine and hypotaurine metabolism, glyoxylate and dicarboxylate metabolism, glycine and serine and threonine metabolism, glycerophospholipid metabolism and primary bile acid biosynthesis, tryosine metabolism), and the increased N-Acetyl-D-galactosamine and the decreased 6-(2-hydroxycyclopentyl) hexanoic acid and nonanoic acid all can disturb the acetyl-CoA formation. Ascorbic acid can form citric acid by oxidation activity, a decrease in the ascorbic acid level may indicate a change in an organism's antioxidant capacity. Succinoadenosine can be degraded and formed from succinic acid by adenosine succinic acid enzymes. Recently, some studies have indicated that the disturbed TCA cycle can result in abnormal lipid metabolism. The increased urinary citric acid excretion has also been reported for obesity accompanied with insulin resistance.⁵⁰ Urinary levels of citric acid were significantly increased in lipid accumulation.⁵¹ Therefore, the increased citric acid, fumaric acid and succinoadenosine in the urine indicated that hyperlipemia disturbed the citric acid, fumaric acid and succinoadenosine entering to the TCA cycle, which resulted that the TCA cycle was disrupted and the lipids were accumulated in the serum and liver in the HF group. The intensity of citric acid statistically decreased in the HF+MG groups compared with the HF group, indicating MG can regulate the hyperlipemia impairment. It may be due to MG can normalize the TCA cycle by regulating its important enzymes (such as, citrate synthase, isocitrate dehydrogenase and α -ketoglutarate dehydrogenase) and can also normalize the TCA cycle by regulating other metabolisms.

The fifth pathway is glycerophospholipid metabolism. Lysophosphatidylcholines (LysoPCs, LPC) is identified in urine in this study, which is the intermediate of glycerophospholipid metabolism. LPC are products or metabolites of phosphatidylcholines (PCs), which are structural components of animal cell membranes. LPC level can be a clinical diagnostic indicator that reveals pathophysiological changes. In the global view, combined with specific TG in the HF rats, the specific molecular lipids were better predictors than HDL-C in the hyperlipemia disease.⁵² LysoPC is present at high concentrations in oxidized LDL, and formed by the reaction of phospholipase A₂.⁵³ About half of the fatty acids in LDL are polyunsaturated fatty acids, mainly linoleic acid with minor amounts of docosahexaenoic acid and arachidonic acid that can be oxidized by a series of factors.⁵⁴ LPC were negatively associated with liver fat and were,

in combination with saturated TG, included in the lipid signature predictive of nonalcoholic fatty-liver disease and liver-fat content. In the present study, the significantly increased LysoPC in the urine in the HF group indicated that hyperlipemia can inhibit lysoPC hydrolases, then resulted the increase LDL concentration in rat serum and lipids accumulation in the liver. Histology observation is confirmed with the LPC levels that the HF group had significantly higher TG, TC, LDL-C levels and lower HDL-C and more liver fatty droplets accumulation than the NC group.

The sixth pathway is primary bile acid biosynthesis. Taurine and glycine is the important intermediate in the bile acid conjugation. Bile acids are amphipathic end products of cholesterol metabolism in the liver, and have different physiological functions. Bile acids can help regulate cholesterol homeostasis and the absorption of lipophilic nutrients in the intestine, and control the glucose, lipid and energy homeostasis.⁵⁵ With continuous increasing HFD intake, the amounts of total bile acids in body fluids will be increased,⁵⁶ because HFD has amount of cholesterol. However, in humans, both taurine and glycine react with bile acids to form a conjugate, taurine is required for bile acid conjugation. Because bile acid conjugates are lost daily in the excreta, considerable amounts of taurine are lost from the body by taurocholic acid. With continuous increasing HFD intake, the level of tauroconjugated bile acids will be increased, and then levels of free taurine will be decreased.⁵⁷ In this study, hyperlipemia can increase the taurine excretion, which indicated that hyperlipemia can result in the increased level of tauroconjugated bile acids. However, the level of taurine in urine increases after MG administration, suggesting that MG can counteract the negative effect of hyperlipemia on taurine formation.

In order to differentiate between diseased and health states, it is a new powerful technology for metabolomics study, which allows for the assessment of global metabolic profiles in easily accessible biofluids and biomarker discovery.^{58,59} Following progress in systems biology, the identification of biomarker patterns and illumination of biochemical processes with the metabolomics using in the postgenomic era has increased contemporaneously.⁶⁰ In this paper, our study indicated an integrated pattern recognition approach to predict MG treatment targets for hyperlipemia by exploring metabolic biomarker and metabolic network. Overall, HFD could result in the hyperlipemia and MG can regulate the hyperlipemia. Schematic overview of the regulation way is shown in Figure 7. Finally, our researches not only indicated that urine metabolomic methods had sufficient sensitivity and specificity to diagnose hyperlipemia and evaluate MG treatment effect on hyperlipemia, but also have the potential to contribute to a further understanding of disease mechanisms. Future researches will be needed to validate the biomarkers which were indicated in the hyperlipemia rats.

5. Conclusions

In this study, a metabolomic approach based on UPLC-ESI-QTOF-MS detection has been successfully established for biomarker exploration in hyperlipemia and mechanism studies of MG. Twenty metabolites were screened out and considered as potential biomarkers of hyperlipemia. Taking these biomarkers as possible drug targets, it is revealed

that MG could reverse the pathological process of hyperlipemia through regulating the disturbed metabolism pathways. TCA cycle, taurine and hypotaurine metabolism, glyoxylate and dicarboxylate metabolism, glycine and serine and threonine metabolism, glycerophospholipid metabolism, primary bile acid biosynthesis were the main perturbed pathways in this pathological process. The identified biomarkers and metabolic networks and give new insights into the pathophysiological changes and molecular mechanisms of hyperlipemia. This is the first study on therapeutic effects of MG in hyperlipemia rats by using urine metabolomics combined with the results of biochemical tests. Of note, the established method indicated MG could provide satisfactory effects on hyperlipemia through regulating the multiple perturbed networks to their normal state.

Acknowledgments

This work was funded by National High Technology Research and Development Program of China (863 program) (2010AA023002) and the National 12th Five-Year Scientific and Technical Support Program of China (2012BAI02B02).

Conflicts of interest

The authors declare that there are no conflicts of interest.

AUTHOR CONTRIBUTIONS

Jun Yin and Chengyan Zhou conceived of the study, designed the experiments, analyzed and interpreted the data and wrote the manuscript. Gang Li, Yanchuan Li, Liya Gong, and Yifan Huang under the direction of Jun Yin developed the metabolic profiling platform, performed mass spectrometry experiments and analyzed the data. Zhiping Shi and Shanshan Du helped in the establishment of the metabolite profiling platform and manuscript revision. Ying Li contributed to data analysis and manuscript generation. Maoqing Wang helped in experimental design, performed statistical analyses and assisted in manuscript generation. Changhao Sun helped in experimental design and manuscript revision, assisted in the interpretation of the data and contributed to manuscript revision.

References

- [1] Chen W, Fan S, Xie X, Xue N, Jin X, Wang L. Novel PPAR Pan Agonist, ZBH Ameliorates Hyperlipidemia and Insulin Resistance in High Fat Diet Induced Hyperlipidemic Hamster. *PLoS One*. 2014 ;9(4):e96056.
- [2] Gupta MA, Knapp K. Cardiovascular and psychiatric morbidity in obstructive sleep apnea (OSA) with insomnia (sleep apnea plus) versus obstructive sleep apnea without insomnia: a case-control study from a Nationally Representative US sample. *PLoS One*. 2014 ;9(3):e90021.
- [3] Vijay-Kumar M, Aitken JD, Carvalho FA, Cullender TC, Mwangi S, Srinivasan S, Sitaraman SV, Knight R, Ley RE, Gewirtz AT. Metabolic syndrome and altered gut microbiota in mice lacking Toll-like receptor 5. *Science*. 2010;328(5975):228-31.
- [4] Nelson ER, Wardell SE, Jasper JS, Park S, Suchindran S, Howe MK, Carver NJ, Pillai RV, Sullivan PM, Sondhi V, Umetani M, Geradts J, McDonnell DP. 27-Hydroxycholesterol links hypercholesterolemia and breast cancer pathophysiology. *Science*. 2013;342(6162):1094-8.
- [5] Niu Y, Li S, Na L, Feng R, Liu L, Li Y, Sun C. Mangiferin decreases plasma free fatty acids through promoting its catabolism in liver by activation of AMPK. *PLoS One*. 2012;7(1):e30782.
- [6] Pardo-Andreu GL, Paim BA, Castilho RF, Velho JA, Delgado R, Vercesi AE, Oliveira HC. *Mangifera indica* L. extract (Vimang) and its main polyphenol mangiferin prevent mitochondrial oxidative stress in atherosclerosis-prone hypercholesterolemic mouse. *Pharmacol Res*. 2008;57(5):332-8.
- [7] E. Holmes, R.L. Loo, J. Stamler, M. Bictash, I.K. Yap, Q. Chan, T. Ebbels, M. De Iorio, I.J. Brown, K.A. Veselkov, M.L. Davignus, H. Kesteloot, H. Ueshima, L. Zhao, J.K. Nicholson, P. Elliott, Human metabolic phenotype diversity and its association with diet and blood pressure, *Nature*. 453(2008) 396-401.
- [8] Tianjiao L, Shuai W, Xiansheng M, Yongrui B, Shanshan G, Bo L, Lu C, Lei W, Xiaorong R. Metabolomics coupled with multivariate data and pathway analysis on potential biomarkers in gastric ulcer and intervention effects of *Corydalis yanhusuo* alkaloid. *PLoS One*. 2014;9(1):e82499.
- [9] A.K. Arakaki, J. Skolnick, J.F. McDonald, Marker metabolites can be therapeutic targets as well, *Nature*. 456(2008) 443.
- [10] A. Sreekumar, L.M. Poisson, T.M. Rajendiran, A.P. Khan, Q. Cao, J. Yu, B. Laxman, R. Mehra, R.J. Lonigro, Y. Li, M.K. Nyati, A. Ahsan, S. Kalyana-Sundaram, B. Han, X. Cao, J. Byun, G.S. Omenn, D. Ghosh, S. Pennathur, D.C. Alexander, A. Berger, J.R. Shuster, J.T. Wei, S. Varambally, C. Beecher, A.M. Chinnaiyan, Metabolomic profiles delineate potential role for sarcosine in prostate cancer progression, *Nature*. 457(2009) 910-914.
- [11] Zhang A, Sun H, Wang X. Potentiating Therapeutic Effects by Enhancing Synergism Based on Active Constituents from Traditional Medicine. *Phytother Res*. 2013. doi: 10.1002/ptr.5032.
- [12] Zhang A, Sun H, Qiu S, Wang X. Advancing Drug Discovery and Development from Active Constituents of Yinchenhao Tang, a Famous Traditional Chinese Medicine Formula. *Evid Based Complement Alternat Med*.

2013;2013:257909.

[13] Wang X, Zhang A, Sun H. Future perspectives of Chinese medical formulae: chinmedomics as an effector. *OMICS*. 2012;16(7-8):414-21.

[14] Sun H, Zhang A, Wang X. Potential role of metabolomic approaches for Chinese medicine syndromes and herbal medicine. *Phytother Res*. 2012;26(10):1466-71.

[15] X. Wang, H. Sun, A. Zhang, W. Sun, P. Wang, Z. Wang, Potential role of metabolomics approaches in the area of traditional Chinese medicine: as pillars of the bridge between Chinese and Western medicine, *J Pharm Biomed Anal*. 55 (2011) 859-868.

[16] Wang X, Zhang A, Yan G, Sun W, Han Y, Sun H. Metabolomics and proteomics annotate therapeutic properties of geniposide: targeting and regulating multiple perturbed pathways. *PLoS One*. 2013;8(8):e71403.

[17] Zhang A, Sun H, Wang Z, Sun W, Wang P, Wang X. Metabolomics: towards understanding traditional Chinese medicine, *Planta Med*. 76(2010)2026-2035.

[18] Ding X, Hu J, Wen C, Ding Z, Yao L, Fan Y. Rapid resolution liquid chromatography coupled with quadrupole time-of-flight mass spectrometry-based metabolomics approach to study the effects of jieduquyuziyin prescription on systemic lupus erythematosus. *PLoS One*. 2014;9(2):e88223.

[19] Liu X, Zhu W, Guan S, Feng R, Zhang H, Liu Q, Sun P, Lin D, Zhang N, Shen J. Metabolomic analysis of anti-hypoxia and anti-anxiety effects of Fu Fang Jin Jing Oral Liquid. *PLoS One*. 2013;8(10):e78281.

[20] Huang D, Yang J, Lu X, Deng Y, Xiong Z, Li F. An integrated plasma and urinary metabonomic study using UHPLC-MS: intervention effects of *Epimedium koreanum* on 'Kidney-Yang Deficiency syndrome' rats. *J Pharm Biomed Anal*. 2013;76:200-6.

[21] Zhao L, Wu H, Qiu M, Sun W, Wei R, Zheng X, Yang Y, Xin X, Zou H, Chen T, Liu J, Lu L, Su J, Ma C, Zhao A, Jia W. Metabolic Signatures of Kidney Yang Deficiency Syndrome and Protective Effects of Two Herbal Extracts in Rats Using GC/TOF MS. *Evid Based Complement Alternat Med*. 2013;2013:540957.

[22] Tan Y, Liu X, Lu C, He X, Li J, Xiao C, Jiang M, Yang J, Zhou K, Zhang Z, Zhang W, Lu A. Metabolic profiling reveals therapeutic biomarkers of processed *Aconitum Carmichaeli* Debx in treating hydrocortisone induced Kidney-Yang deficiency syndrome rats. *J Ethnopharmacol*. 2014. pii: S0378-8741(14)00112-3.

[23] Zou HB, Han ZF, Zhai H, Wei YQ, Wang F. The first and second cluster analysis of dual index grade sequence of IR fingerprint spectra of Guifudihuang pill and Jinkuishenqi pill samples and their quality evaluation. *Guang Pu Xue Yu Guang Pu Fen Xi*. 2007;27(12):2432-6.

[24] X. Liang, X. Chen, Q. Liang, H. Zhang, P. Hu, Y. Wang, G. Luo, Metabonomic study of Chinese medicine Shuanglong formula as an effective treatment for myocardial infarction in rats. *J Proteome Res*. 10(2011)790-799.

[25] Li B, Luo QL, Nurahmat M, Jin HL, Du YJ, Wu X, Lv YB, Sun J, Abduwaki M, Gong WY, Dong JC. Establishment and comparison of combining disease and syndrome model of asthma with "kidney yang deficiency"

and "abnormal savda". *Evid Based Complement Alternat Med.* 2013;2013:658364.

[26] Randhawa M, Sangar V, Tucker-Samaras S, Southall M. Metabolic signature of sun exposed skin suggests catabolic pathway overweighs anabolic pathway. *PLoS One.* 2014;9(3):e90367.

[27] Caporaso JG, Kuczynski J, Stombaugh J, Bittinger K, Bushman FD, Costello EK, Fierer N, Peña AG, Goodrich JK, Gordon JI, Huttley GA, Kelley ST, Knights D, Koenig JE, Ley RE, Lozupone CA, McDonald D, Muegge BD, Pirrung M, Reeder J, Sevinsky JR, Turnbaugh PJ, Walters WA, Widmann J, Yatsunenko T, Zaneveld J, Knight R. QIIME allows analysis of high-throughput community sequencing data. *Nat Methods.* 2010;7(5):335-6.

[28] Gwacham N1, Wagner DR. Acute effects of a caffeine-aurine energy drink on repeated sprint performance of American college football players. *Int J Sport Nutr Exerc Metab.* 2012;22(2):109-16.

[29] Schaffer SW1, Shimada K, Jong CJ, Ito T, Azuma J, Takahashi K. Effect of taurine and potential interactions with caffeine on cardiovascular function. *Amino Acids.* 2014;46(5):1147-57.

[30] Alvarez JG, Storey BT. Taurine, hypotaurine, epinephrine and albumin inhibit lipid peroxidation in rabbit spermatozoa and protect against loss of motility. *Biol Reprod.* 1983;29(3):548-55.

[31] Li M1, Reynolds CM, Sloboda DM, Gray C, Vickers MH. Effects of taurine supplementation on hepatic markers of inflammation and lipid metabolism in mothers and offspring in the setting of maternal obesity. *PLoS One.* 2013;8(10):e76961.

[32] Murakami S1, Kondo Y, Toda Y, Kitajima H, Kameo K, Sakono M, Fukuda N. Effect of taurine on cholesterol metabolism in hamsters: up-regulation of low density lipoprotein (LDL) receptor by taurine. *Life Sci.* 2002;70(20):2355-66.

[33] Zhang M1, Bi LF, Fang JH, Su XL, Da GL, Kuwamori T, Kagamimori S. Beneficial effects of taurine on serum lipids in overweight or obese non-diabetic subjects. *Amino Acids.* 2004;26(3):267-71.

[34] Worden JA, Stipanuk MH. A comparison by species, age and sex of cysteinesulfinate decarboxylase activity and taurine concentration in liver and brain of animals. *Comp Biochem Physiol B.* 1985;82(2):233-9.

[35] Stapleton PP1, Charles RP, Redmond HP, Bouchier-Hayes DJ. Taurine and human nutrition. *Clin Nutr.* 1997;16(3):103-8.

[36] Tsuboyama-Kasaoka N1, Shozawa C, Sano K, Kamei Y, Kasaoka S, Hosokawa Y, Ezaki O. Taurine (2-aminoethanesulfonic acid) deficiency creates a vicious circle promoting obesity. *Endocrinology.* 2006;147(7):3276-84.

[37] Turnbaugh PJ1, Ley RE, Mahowald MA, Magrini V, Mardis ER, Gordon JI. An obesity-associated gut microbiome with increased capacity for energy harvest. *Nature.* 2006;444(7122):1027-31.

[38] Dumas ME1, Barton RH, Toye A, Cloarec O, Blancher C, Rothwell A, Fearnside J, Tatoud R, Blanc V, Lindon JC, Mitchell SC, Holmes E, McCarthy MI, Scott J, Gauguier D, Nicholson JK. Metabolic profiling reveals a contribution of gut microbiota to fatty liver phenotype in insulin-resistant mice. *Proc Natl Acad Sci U S A.*

2006;103(33):12511-6.

[39] Al Rajabi A1, Castro GS, da Silva RP, Nelson RC, Thiesen A, Vannucchi H, Vine DF, Proctor SD, Field CJ, Curtis JM, Jacobs RL. Choline supplementation protects against liver damage by normalizing cholesterol metabolism in *Pemt/Ldlr* knockout mice fed a high-fat diet. *J Nutr*. 2014;144(3):252-7.

[40] Amelio I1, Cutruzzolá F2, Antonov A3, Agostini M3, Melino G4. Serine and glycine metabolism in cancer. *Trends Biochem Sci*. 2014;39(4):191-8.

[41] Jain M1, Nilsson R, Sharma S, Madhusudhan N, Kitami T, Souza AL, Kafri R, Kirschner MW, Clish CB, Mootha VK. Metabolite profiling identifies a key role for glycine in rapid cancer cell proliferation. *Science*. 2012;336(6084):1040-4.

[42] Renwick SB1, Snell K, Baumann U. The crystal structure of human cytosolic serine hydroxymethyltransferase: a target for cancer chemotherapy. *Structure*. 1998;6(9):1105-16.

[43] Yamashina S1, Ikejima K, Enomoto N, Takei Y, Sato N. Glycine as a therapeutic immuno-nutrient for alcoholic liver disease. *Alcohol Clin Exp Res*. 2005;29(11 Suppl):162S-5S.

[44] KAWAKAMI T, TOKUDA R. Relation between fatty liver due to cystine and methionine and glycine. *Keio J Med*. 1962;39:75-7.

[45] Swann JR1, Tuohy KM, Lindfors P, Brown DT, Gibson GR, Wilson ID, Sidaway J, Nicholson JK, Holmes E. Variation in antibiotic-induced microbial recolonization impacts on the host metabolic phenotypes of rats. *J Proteome Res*. 2011;10(8):3590-603.

[46] Delaney J1, Neville WA, Swain A, Miles A, Leonard MS, Waterfield CJ. Phenylacetyl-glycine, a putative biomarker of phospholipidosis: its origins and relevance to phospholipid accumulation using amiodarone treated rats as a model. *Biomarkers*. 2004;9(3):271-90.

[47] Fallarino F1, Grohmann U, Hwang KW, Orabona C, Vacca C, Bianchi R, Belladonna ML, Fioretti MC, Alegre ML, Puccetti P. Modulation of tryptophan catabolism by regulatory T cells. *Nat Immunol*. 2003;4(12):1206-12.

[48] Moffett JR1, Namboodiri MA. Tryptophan and the immune response. *Immunol Cell Biol*. 2003;81(4):247-65.

[49] Meléndez-Hevia E1, Waddell TG, Cascante M. The puzzle of the Krebs citric acid cycle: assembling the pieces of chemically feasible reactions, and opportunism in the design of metabolic pathways during evolution. *J Mol Evol*. 1996;43(3):293-303.

[50] Jones JG1, Sherry AD, Jeffrey FM, Storey CJ, Malloy CR. Sources of acetyl-CoA entering the tricarboxylic acid cycle as determined by analysis of succinate ¹³C isotopomers. *Biochemistry*. 1993;32(45):12240-4.

[51] Yuan LQ1, Lu Y, Luo XH, Xie H, Wu XP, Liao EY. Taurine promotes connective tissue growth factor (CTGF) expression in osteoblasts through the ERK signal pathway. *Amino Acids*. 2007;32(3):425-30.

[52] Yuan LQ1, Xie H, Luo XH, Wu XP, Zhou HD, Lu Y, Liao EY. Taurine transporter is expressed in osteoblasts. *Amino Acids*. 2006;31(2):157-63

- [53] Takabe W1, Kanai Y, Chairoungdua A, Shibata N, Toi S, Kobayashi M, Kodama T, Noguchi N. Lysophosphatidylcholine enhances cytokine production of endothelial cells via induction of L-type amino acid transporter 1 and cell surface antigen 4F2. *Arterioscler Thromb Vasc Biol.* 2004;24(9):1640-5.
- [54] Mertens A1, Holvoet P. Oxidized LDL and HDL: antagonists in atherothrombosis. *FASEB J.* 2001;15(12):2073-84.
- [55] Li T1, Chiang JY. Bile Acid signaling in liver metabolism and diseases. *J Lipids.* 2012;2012:754067.
- [56] Hofmann AF. The continuing importance of bile acids in liver and intestinal disease. *Arch Intern Med.* 1999;159(22):2647-58.
- [57] Obinata K1, Maruyama T, Hayashi M, Watanabe T, Nittono H. Effect of taurine on the fatty liver of children with simple obesity. *Adv Exp Med Biol.* 1996;403:607-13.
- [58] Zhang A, Zhou X, Zhao H, Guan Y, Zhou S, Yan GL, Ma Z, Liu Q, Wang X. Rapidly improved determination of metabolites from biological data sets using the high-efficient TransOmics tool. *Mol Biosyst.* 2014;10(8):2160-5.
- [59] Zhang A, Sun H, Yan G, Wang P, Han Y, Wang X. Metabolomics in diagnosis and biomarker discovery of colorectal cancer. *Cancer Lett.* 2014;345(1):17-20.
- [60] Zhang A, Sun H, Wang X. Urinary metabolic profiling of rat models revealed protective function of scoparone against alcohol induced hepatotoxicity. *SCIENTIFIC REPORTS.* 2014, DOI: 10.1038/srep06768.

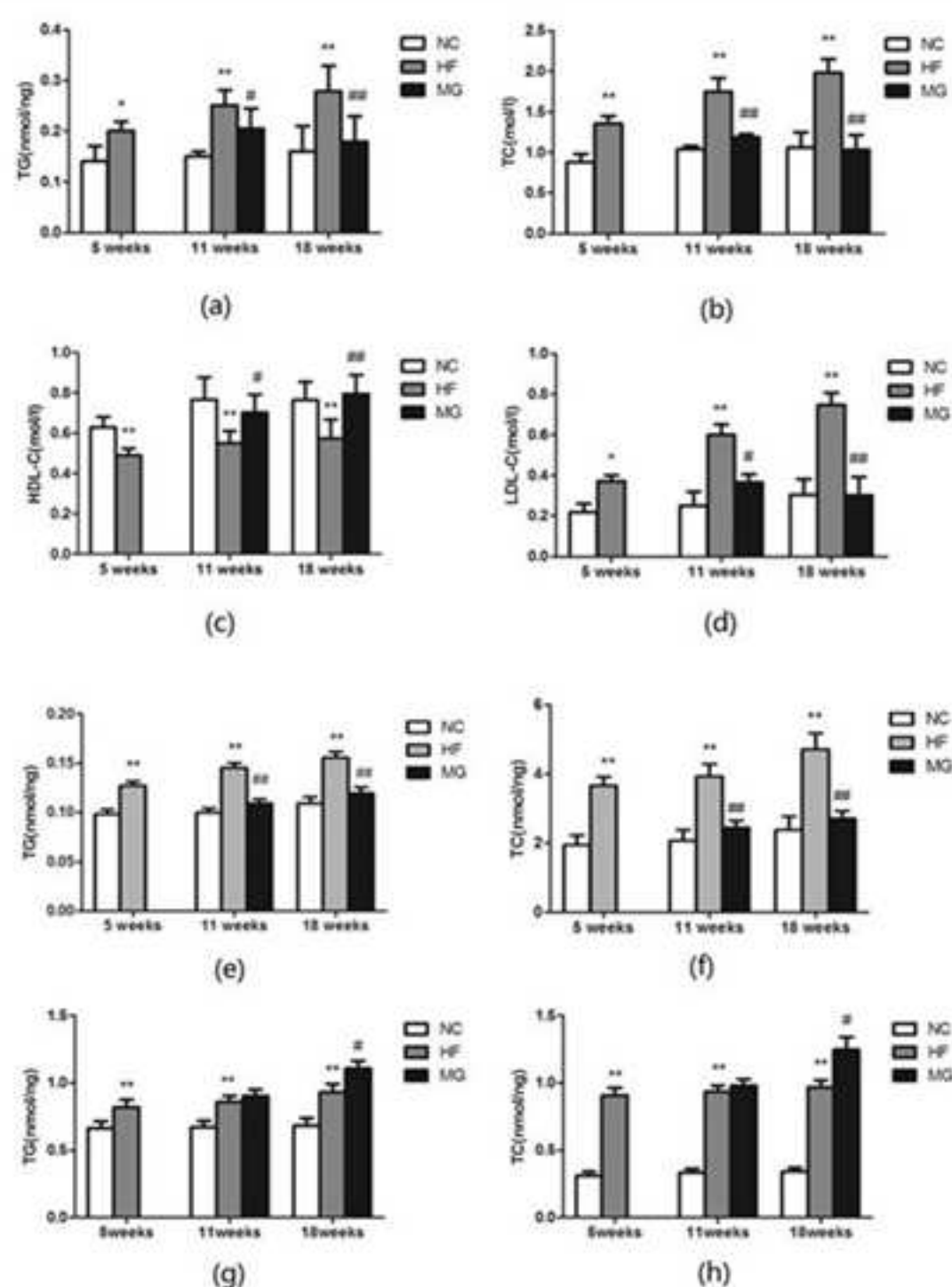


Figure 1. (a-d) Effect of MG on serum metabolites. (a) TG, (b) TC, (c) HDL-C, (d) LDL-C. (e-h) Effect of mangiferin on liver TG, TC and fecal TG, TC. (e) Liver TG, (f) TC at 5, 11, 18 weeks; Faces (g) TG, (h) TC at the 5, 11, 18 weeks. The values are expressed as mean \pm SD. In the 5th wk, NC(n=6): normal control group, HF(n=6): high-fat control group; In the 11th wk, NC(n=6): normal control group, HF(n=6): high-fat control group, HF+MG (n=6): high-fat diet+ Mangiferin (300mg/kg BW). In the 18th wk, NC (n=8): normal control group, HF (n=14): high-fat control group, HF+MG (n=14): high-fat diet+Mangiferin (300mg/kg BW) . *P<0.05 and **P<,0.01 indicate statistically significant differences when compared with the normal control group. #P<0.05 and ##P<0.01 indicate statistically significant differences when compared high-fat control group.

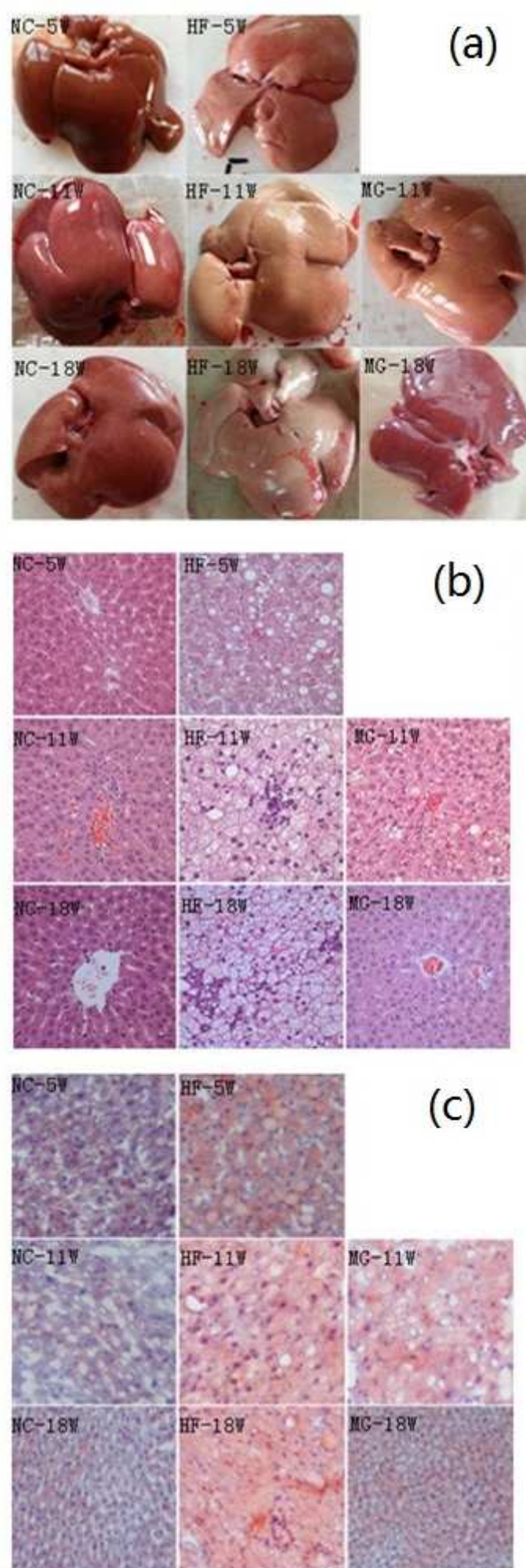


Figure 2. (a-c) Effects of mangiferin on lipid accumulation in the liver and kidney. (a) Macroscopic images of liver, (b) liver sections stained with H&E and (c) oil red at 5, 11, 18weeks.

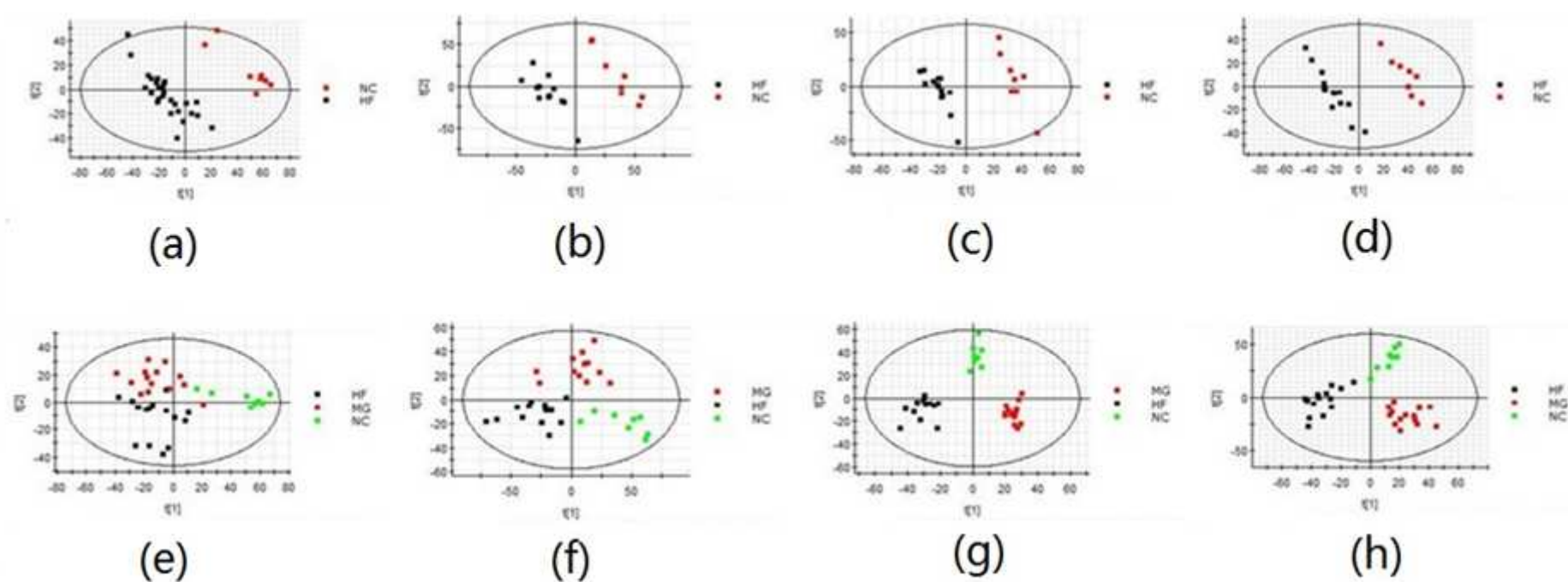


Figure 3. Partial least-squares discriminant analysis (PLS-DA) score plots of rats in the ESI+ in the NC group and HF group. (a) At Week 5, $n = 8(\text{NC}), 28(\text{HF})$ (for two components, $R^2Y = 0.9463$, $Q^2 = 0.7719$); (b) At week 10, $n = 8(\text{NC}), 14(\text{HF})$ (for two components $R^2Y = 0.9634$, $Q^2 = 0.8215$); and (c) At week 14, $n = 8(\text{NC}), 14(\text{HF})$ (for one component $R^2Y = 0.9205$, $Q^2 = 0.7782$); (d) At week 18, $n = 8(\text{NC}), 14(\text{HF})$ (for two components $R^2Y = 0.9822$, $Q^2 = 0.8264$). (e-h) Partial least-squares discriminant analysis (PLS-DA) score plots of rats in the ESI+ in the NC group, HF group and MG group. (e) Weeks 5 (before MG supplementation), $n = 8(\text{NC}), 14(\text{HF}), 14(\text{HF}+\text{MG})$ (for two components, $R^2Y = 0.6536$, $Q^2 = 0.1974$); (f) weeks 10 (after MG supplementation for 5 weeks), $n = 8(\text{NC}), 14(\text{HF}), 14(\text{HF}+\text{MG})$ (for three components $R^2Y = 0.8744$, $Q^2 = 0.6729$); (g) weeks 14 (after MG supplementation for 9 weeks), $n = 8(\text{NC}), 14(\text{HF}), 14(\text{HF}+\text{MG})$ (for two components $R^2Y = 0.8756$, $Q^2 = 0.7512$); (h) weeks 18 (after MG supplementation for 13 weeks), $n = 8(\text{NC}), 14(\text{HF}), 14(\text{HF}+\text{MG})$ ($R^2Y = 0.8575$, $Q^2 = 0.7083$).

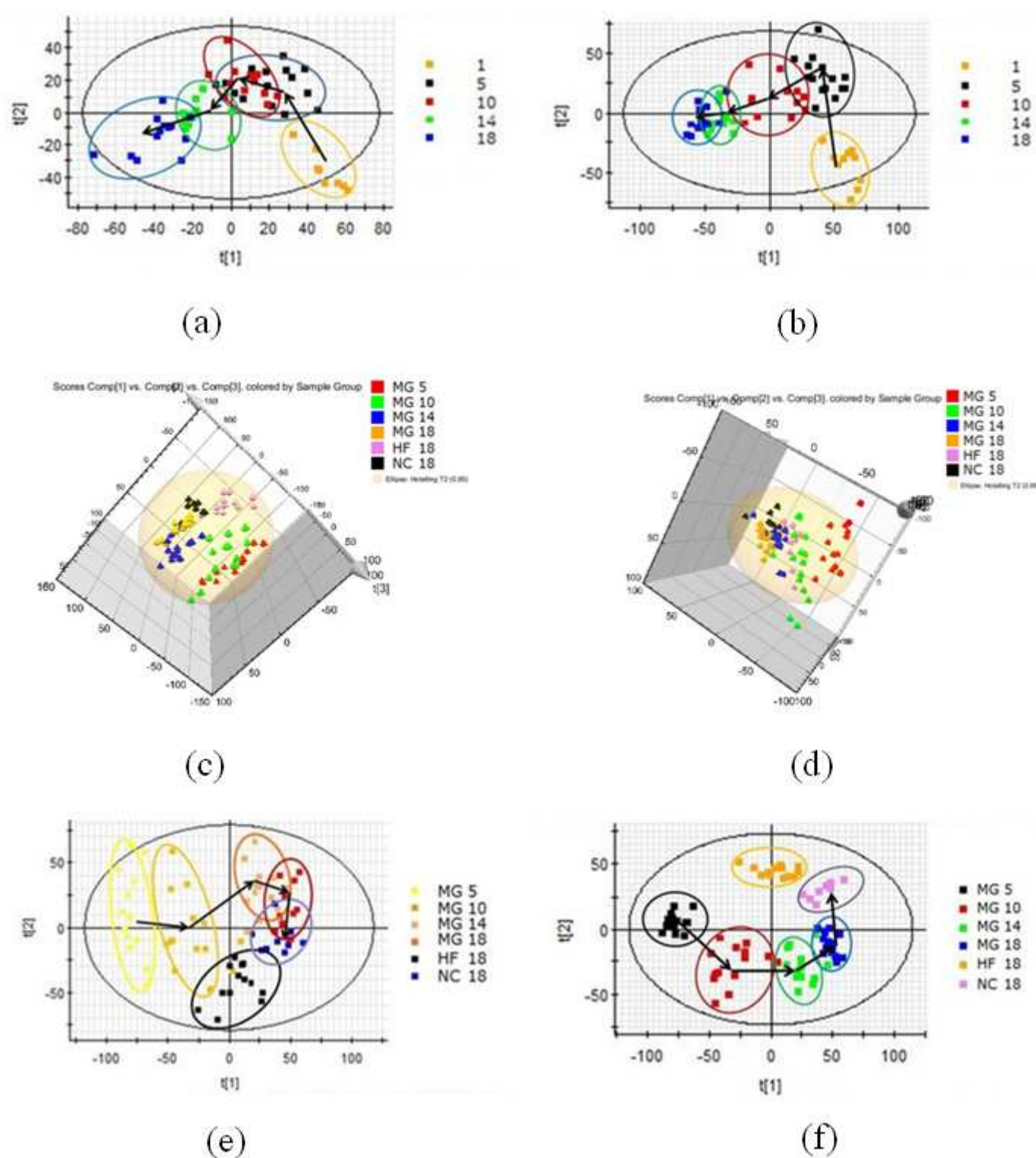


Figure 4. (a-b) Partial least-squares discriminant analysis (PLS-DA) score plots model in the (a) ESI^+ and (b) ESI^- derived from the urine of rats on high fat diet. Samples were collected during weeks 1 to 18. Yellow star(1): weeks 1 to 5; Black star(5): weeks 6 to 10; red star(10): weeks 11 to 14; Green star(14): weeks 15 to 18. (c-d) 3-D metabolic trajectory scores plots of PCA model for the NC, HF, HF+MG groups in the (c) ESI^+ and (d) ESI^- . Samples were collected during 0-13 weeks after MG supplementation. MG 5: weeks 0; MG10: weeks 5; HF+MG 14: weeks 9; MG 18: weeks 13; HF 18; weeks 18; NC 18: weeks 18. (e-f) Partial least-squares discriminant analysis (PLS-DA) score plots model in the (e) ESI^+ and (f) ESI^- derived from the urine of rats on high fat diet after MG supplementation. Samples were collected during 0-13 weeks after MG supplementation. MG5: weeks 0; MG10: weeks 5; MG14: weeks 9; MG 18: weeks 13; HF 18: weeks 18; NC 18: weeks 18.

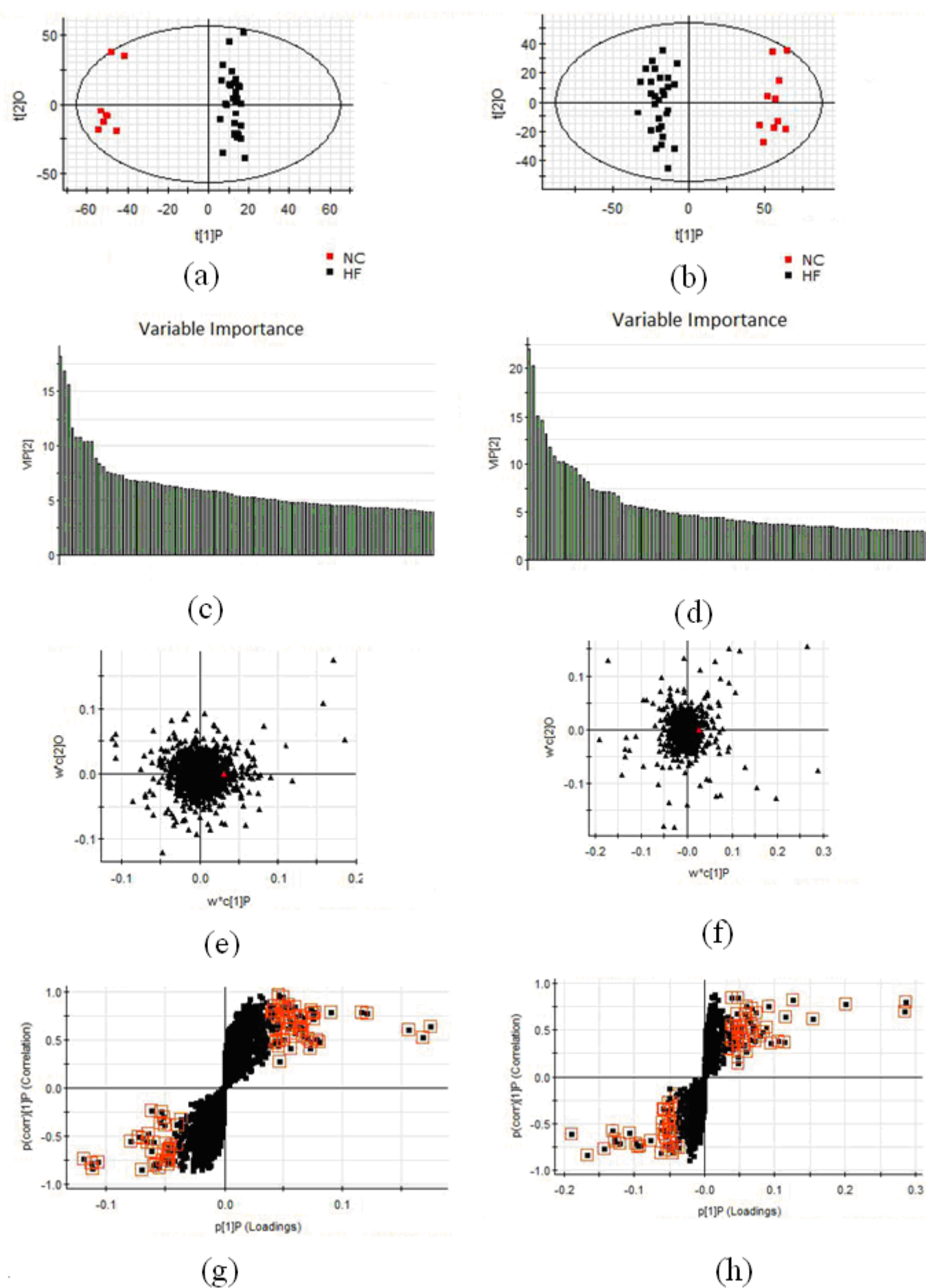


Figure 5. (a-b) OPLS-DA score plots resulting in the (a) ESI⁺ and (b) ESI⁻ from the LC/MS spectra of NC and HF at the 5 weeks. (c,d) VIP plot of NC vs HF in the (c) ESI⁺ and (d) ESI⁻ at the 5 weeks. (e,f) Loading plot of OPLS-DA of hyperlipemia in the (e) ESI⁺ and (f) ESI⁻ at the 5 weeks. (g,h) S-plot of OPLS-DA of hyperlipemia in the (g) ESI⁺ and (h) ESI⁻ at the 5 weeks.

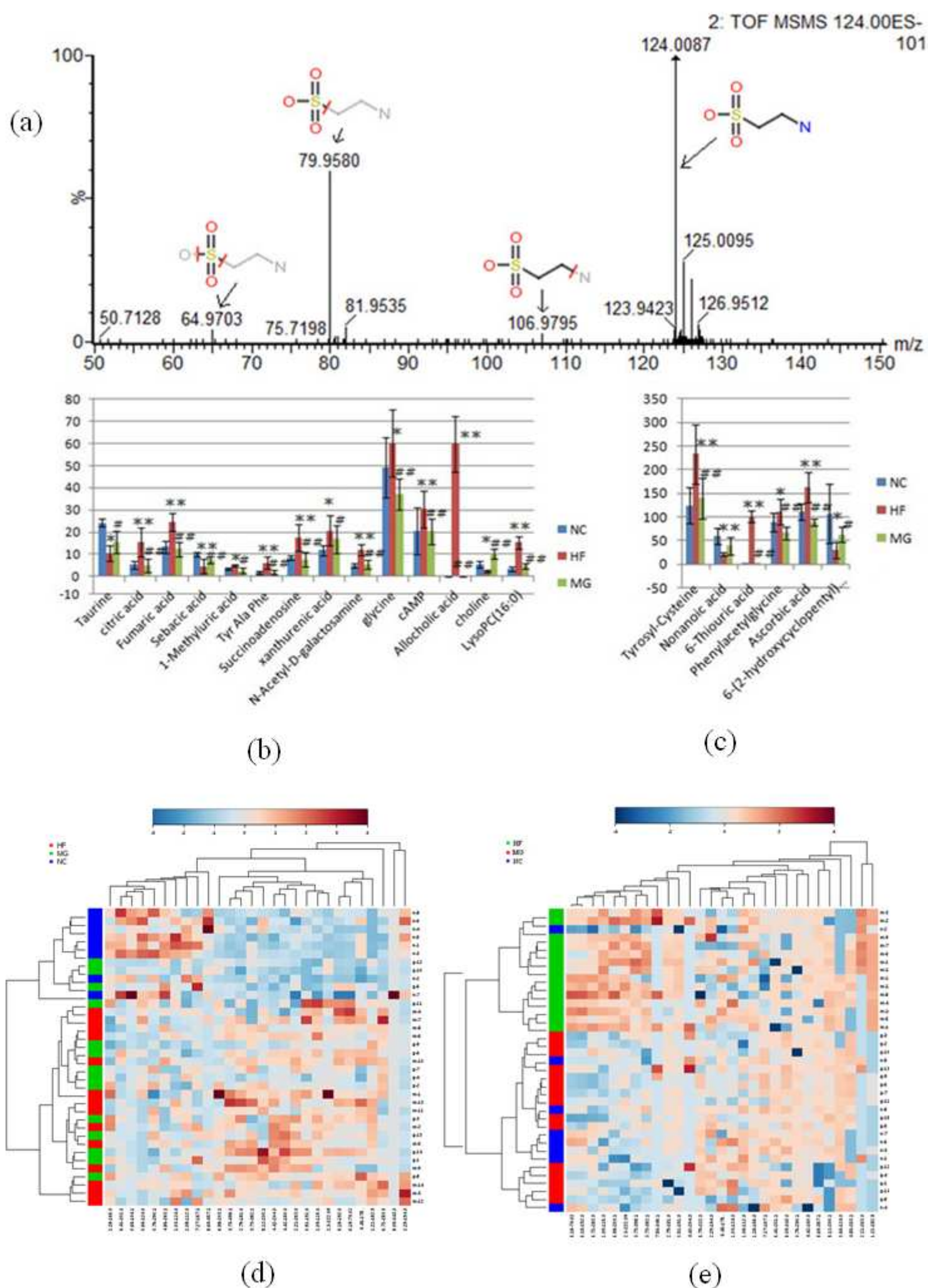


Figure 6. (a) Chemical structure and mass fragment information of taurine in ESI-mode. (b-c) Changes in the relative concentrations of target metabolites identified in different groups. The corresponding markers represented to the Table 1. A two-tailed, parametric t-test was used to determine the significance of the change in relative concentrations for each metabolite. Bars represent the mean relative metabolite concentration and standard deviations. * $p < 0.05$; ** $p < 0.001$. (d-e) Heatmap is commonly used for unsupervised clustering. Agglomerative hierarchical clustering begins with each sample as separate cluster and then proceeds to combine them until all samples belong to one cluster. The result is usually presented as a heatmap that have been implemented in MetaboAnalyst. Rows: samples; Columns: metabolites; Color key indicates metabolite expression value. The NC group rats are indicated by blue, the HF group rats by red, and the MG group by green.

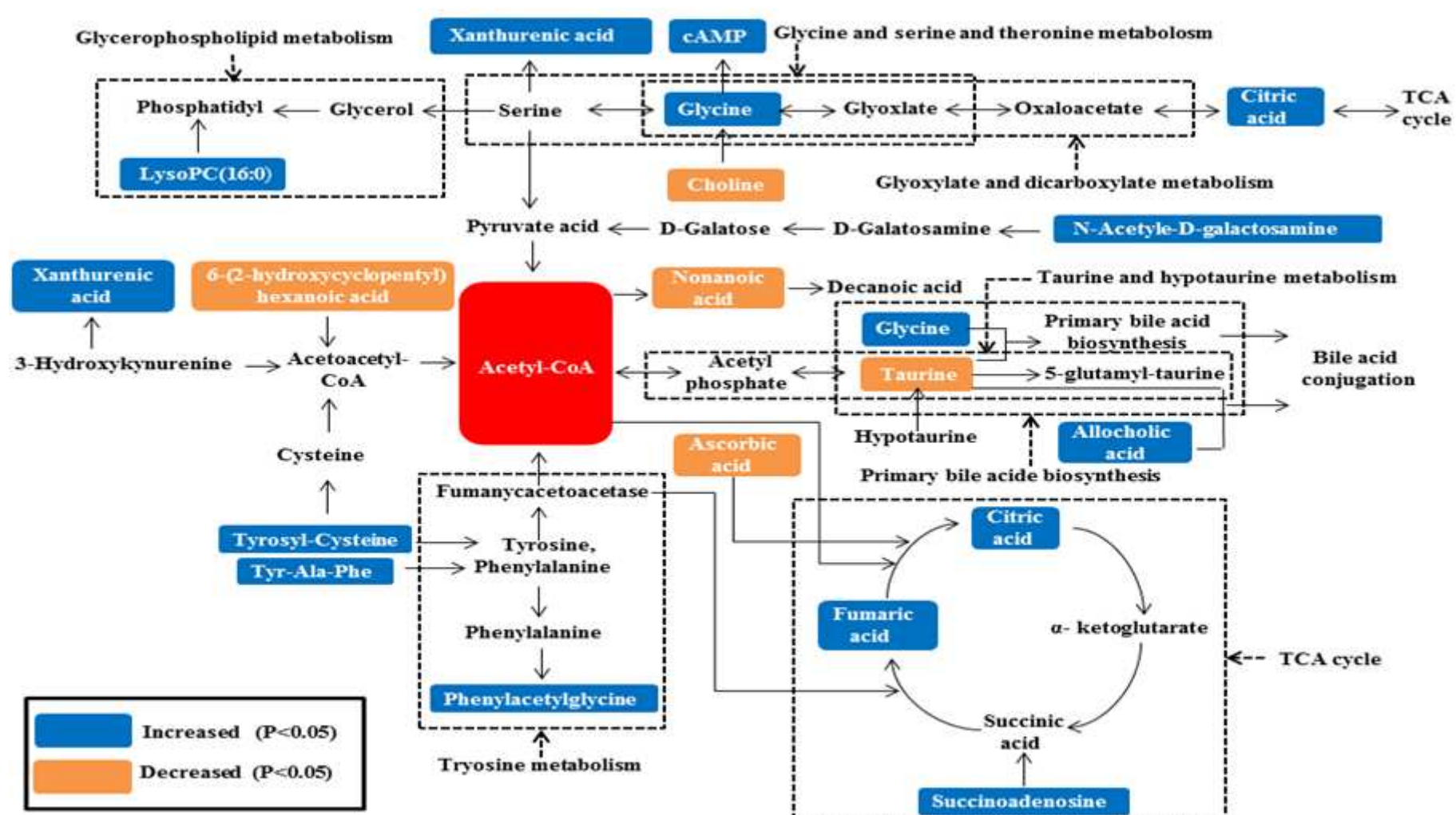
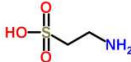
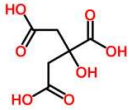
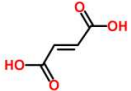
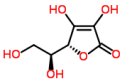
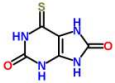
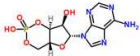
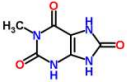
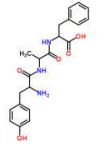
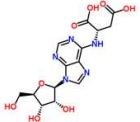
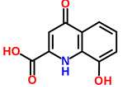
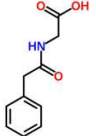
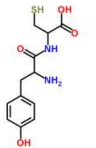
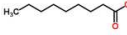


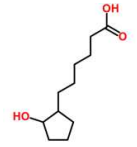
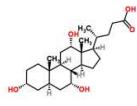
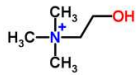
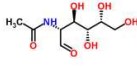
Figure 7. Schematic overview of the metabolites and relevant pathways changing for CC modulation according to the KEGG PATHWAY database. The important correlation networks of the potential biomarkers in the experiment. Metabolites with blue dashed area present significant increase in HF group compared to NC group and HF+MG group. Metabolites with yellow area present significant decrease in HF group compared to NC group and HF+MG group.

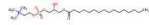
Table 1. Potential biomarkers identified and changing trends of hyperlipemia rats in ESI⁺ and ESI⁻ model

No.	Time	ppm	Mass	Calc. Mass	[M+H] ⁺ / [M-H] ⁻	Formula	Identified	MS/MS	Trend	Structure
1	0.66	-3.2	124.0064	124.0068	[M-H] ⁻	C ₂ H ₆ NO ₃ S	Taurine	124[M-H]- 106[M-H-NH ₃]- 95[M-H-CH ₃ N]- 80[M-H-C ₂ H ₆ N]- 65[M-H-C ₂ H ₅ NO]- 191[M-H]-, 173[M-H-H ₂ O]-, 155 [M-H-H ₄ O ₂]- 129[M-H-CH ₂ O ₃]- 111[M-H-CH ₄ O ₄]- 85[M-H-C ₂ H ₂ O ₅]- 73[M-H-C ₃ H ₂ O ₅]- 115[M-H]- 87[M-H-CO]- 71[M-H-CO ₂]- 59[M-H-CO-CO ₂]- 175[M-H]-, 115[M-H-C ₂ H ₄ O ₂]- 87[M-H-C ₃ H ₄ O ₃]- 71[M-H-C ₃ H ₄ O ₄]- 59[M-H-C ₄ H ₄ O ₄]-	↓	
2	0.91	-1.0	191.0990	191.0192	[M-H] ⁻	C ₆ H ₇ O ₇	Citric acid	129[M-H-CH ₂ O ₃]- 111[M-H-CH ₄ O ₄]- 85[M-H-C ₂ H ₂ O ₅]- 73[M-H-C ₃ H ₂ O ₅]- 115[M-H]- 87[M-H-CO]- 71[M-H-CO ₂]- 59[M-H-CO-CO ₂]- 175[M-H]-, 115[M-H-C ₂ H ₄ O ₂]- 87[M-H-C ₃ H ₄ O ₃]- 71[M-H-C ₃ H ₄ O ₄]- 59[M-H-C ₄ H ₄ O ₄]-	↑	
3	1.09	0	115.0031	115.0031	[M-H] ⁻	C ₄ H ₃ O ₄	Fumaric acid	115[M-H-C ₂ H ₄ O ₂]- 87[M-H-C ₃ H ₄ O ₃]- 71[M-H-C ₃ H ₄ O ₄]- 59[M-H-C ₄ H ₄ O ₄]-	↑	
4	1.09	-4.0	175.0236	175.0243	[M-H] ⁻	C ₆ H ₇ O ₆	Ascorbic acid	115[M-H-C ₂ H ₄ O ₂]- 87[M-H-C ₃ H ₄ O ₃]- 71[M-H-C ₃ H ₄ O ₄]- 59[M-H-C ₄ H ₄ O ₄]-	↑	

5	1.21	3.8	182.9984	182.9977	[M-H] ⁻	C ₅ H ₃ N ₄ O ₂ S	6-Thiouric acid	182[M-H]- 96 [M-H-C ₃ NOS]-	↑	
6	2.57	-0.9	328.0444	328.0447	[M-H] ⁻	C ₁₀ H ₁₁ N ₅ O ₆ P	cAMP	328[M-H]-, 134[M-H-C ₅ H ₇ O ₆ P]- 96 [M-H-C ₄ H ₇ N ₂ O ₅ P]- 78[M-H-C ₁₀ H ₁₁ N ₅ O ₃]- 181[M-H]-, 168[M-H-N]- 138[M-H-CHNO]-	↑	
7	2.79	5.0	181.0371	181.0362	[M-H] ⁻	C ₆ H ₅ N ₄ O ₃	1-Methyluric acid	122[M-H-CH ₃ N ₂ O]- 108[M-H-C ₂ H ₅ N ₂ O]- 96[M-H-C ₃ H ₄ N ₂ O]- 94[M-H-C ₂ H ₃ N ₂ O ₂]- 83[M-H-C ₃ H ₂ N ₂ O ₂]- 398[M-H]-, 380[M-H-H ₂ O]-,	↑	
8	3.73	-4.0	398.1700	398.1716	[M-H] ⁻	C ₂₁ H ₂₄ N ₃ O ₅	Tyr Ala Phe	250[M-H -C ₉ H ₁₀ NO]-, 153[M-H-C ₁₅ H ₁₉ NO ₂]- 114[M-H-C ₁₇ H ₁₈ NO ₃]-, 382[M-H]-, 346[M-H-2H ₂ O]-	↑	
9	3.73	1.0	382.1003	382.0999	[M-H] ⁻	C ₁₄ H ₁₆ N ₅ O ₈	Succinoadenosine	316[M-H-2H ₂ O-OCH ₂]- 250[M-H-C ₅ H ₈ O ₄]- 206[M-H-C ₅ H ₈ O ₄ -CO ₂]-	↑	

10	4.42	-3.1	204.0288	204.0297	[M-H] ⁻	C ₁₀ H ₇ NO ₄	Xanthurenic acid	115[M-H-C ₁₀ H ₁₃ N ₅ O ₄]- 97[M-H-C ₁₀ H ₁₃ N ₅ O ₄ -H ₂ O]- 71[M-H-C ₁₀ H ₁₃ N ₅ O ₄ -CO ₂]- 204[M-H]- 160[M-H-CO ₂]- 132[M-H-CO ₂ -CO]- 125[M-H-CH ₃ O ₄]- 116[M-H-C ₂ H ₂ NO ₃]-	↑	
11	6.18	-3.1	192.0655	192.0661	[M-H] ⁻	C ₁₀ H ₁₀ NO ₃	Phenylacetyl-glycine	192[M-H]-, 74[M-H-C ₈ H ₆ O]-	↑	
12	6.18	0	74.0242	74.0242	[M-H] ⁻	C ₂ H ₄ NO ₂	Glycine	74[M-H]- 58[M-H-NH ₂]-	↑	
13	6.71	-3.2	283.0744	283.0753	[M-H] ⁻	C ₁₂ H ₁₅ N ₂ O ₄ S	Tyrosyl-Cysteine	283[M-H]-, 265[M-H-H ₂ O]-, 221[M-H-COOH-OH]-, 175[M-C ₇ H ₈ O]-, 157[M-C ₇ H ₈ O-H ₂ O]-, 129[M-C ₈ H ₁₀ O ₃]-, 157[M-H]-	↑	
14	7.27	3.2	157.1234	157.1229	[M-H] ⁻	C ₉ H ₁₇ O ₂	Nonanoic acid	139[M-H-H ₂ O]- 127[M-H-C ₂ H ₆]- 111[M-H-CH ₂ O ₂]-	↓	

15	8.07	2.5	199.1339	199.1334	[M-H] ⁻	C ₁₁ H ₁₉ O ₃	6-(2-hydroxycyclopentyl) hexanoic acid	99[M-H-C ₄ H ₁₀]- 85[M-H-C ₅ H ₁₂]- 71[M-H-C ₆ H ₁₄]- 57[M-H-C ₇ H ₁₆]- 199[M-H]-, 155[M-H-CO ₂]-, 140[M-H-C ₂ H ₃ O ₂]-, 112[M-H-C ₂ H ₃ O ₂ -CO ₂]-	↓	
16	8.86	-4.4	407.2779	407.2797	[M-H] ⁻	C ₂₄ H ₃₉ O ₅	Allocholic acid	407[M-H]-, 389[M-H-H ₂ O]-, 361[M-H-H ₂ O-CO ₂],	↑	
17	0.66	-5.8	104.1069	104.1075	[M+H] ⁺	C ₅ H ₁₄ NO	Choline	104[M]+, 60[M-3CH ₃]+	↓	
18	2.3	-0.5	222.0977	222.0978	[M+H] ⁺	C ₈ H ₁₆ NO ₆	N-Acetyl-D-galactosamine	222[M+H]+, 205[M+H-H ₂ O]+, 145[M+H-C ₂ H ₅ O ₃], 127[M+H-C ₂ H ₅ O ₃ -H ₂ O]+, 203[M+H]+, 143[M+H-C ₂ H ₄ O ₂]+, 125[M+H-CH ₂ O ₄]+, 97[M+H-C ₃ H ₆ O ₄]+, 83[M+H-C ₄ H ₈ O ₄]+, 69[M+H-C ₆ H ₁₄ O ₃]+,	↑	
19	6.98	-1.5	203.1280	203.1283	[M+H] ⁺	C ₁₀ H ₁₉ O ₄	Sebacic acid	125[M+H-CH ₂ O ₄]+, 97[M+H-C ₃ H ₆ O ₄]+, 83[M+H-C ₄ H ₈ O ₄]+, 69[M+H-C ₆ H ₁₄ O ₃]+,	↓	

20	10.31	4.8	496.3427	496.3403	[M] ⁺	C ₂₄ H ₅₁ NO ₇ P	LysoPC(16:0)	496[M] ⁺ , 478[M-H ₂ O] ⁺ , 258[M-C ₁₀ H ₂₅ NO ₃ P] ⁺ , 184[M-C ₁₃ H ₃₁ NO ₅ P] ⁺ ,	↑	
----	-------	-----	----------	----------	------------------	---------------------------------------------------	--------------	-----------------------------------------------------------------------------------------------------------------------------------------------------------------------------------------------------------------------	---	-------------------------------------------------------------------------------------
